The Global Forecast System Model Instability Issue and Potential Solutions

Xiaqiong Zhou[1] and Hann-Ming Henry Juang[2]
[1]CPAESS UCAR at GFDL/NOAA, Princeton, NJ [2]EMC NCEP/NOAA, College Park, MD
Email: Xiaqiong.Zhou@noaa.gov and henry.juang@noaa.gov

1. Introduction

The Global Forecast System (GFS) was updated from version 15 to 16 on 22 March, 2021. GFS.v16 has its number of vertical layers increased from 64 to 127 and model top extended from 54 km to 80 km. Physics parameterizations in GFS.v16 were also improved. It is the first major upgrade to the Finite-Volume Cubed-Sphere (FV3) dynamical core-based GFS (Lin and Rood, 1997; Putman and Lin, 2007) since its implementation for operation in 2019. Retrospective and real-time experiments were performed to evaluate the model performances. However, GFS.v16 encountered a few model instability failures from real-time parallel experiments. The diagnosis of these cases and the solutions proposed to remove the numerical instability are summarized in this study.

2. Diagnosis of failed cases

There were nine failed cases in total from the GFS.v16 real-time parallel experiment. The model integration was interrupted when the pressure thickness of a certain layer became negative or the thickness expressed in height became NaN (not-a-number). It was found that all these cases failed over a land grid when a strong tropical cyclone approached from the east. For example, the case initialized at 18Z UTC on 22 July 2020 failed when the eyewall of a strong tropical cyclone reached the Philippine east coast with strong onshore winds of about 40-50 m/s. By examining the model prognostic variables at each acoustic time step (12.5s), we found that the upward motion at lower levels at the grid points in question increased with time and then abruptly changed to unrealistically strong downdrafts (>300m/s) before the model crashed.

In the FV3 dynamic core for GFS.v16, the pressure perturbation p' and vertical velocity w tendency equations solved in a semi-implicit time-difference scheme are transformed to a tridiagonal matrix system of equations for w. This system requires coefficients and weights related to p' and layer thickness δz to solve w using the Thomas algorithm. In the corresponding subroutine for the non-hydrostatic adjustment, the layer-mean non-hydrostatic pressure perturbation is calculated first with $p' = p - p^*$, where p^* is hydrostatic pressure and p is full pressure, and can be calculated from the ideal gas law:

$$p = \exp\left\{\gamma log\left(-R_d \theta_v \frac{\partial m}{\partial z}\right)\right\} \qquad (1)$$

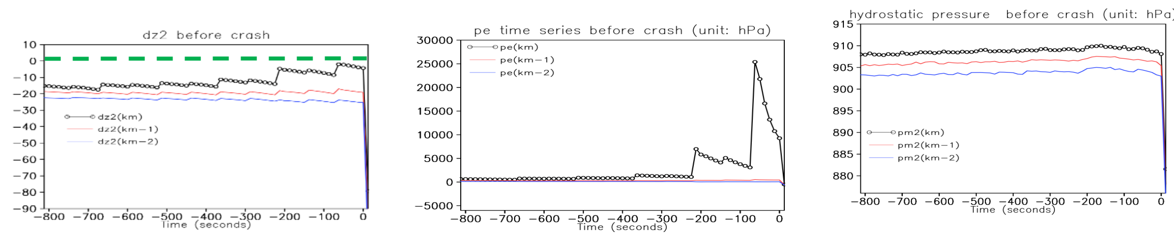

Figure 1. The time series of δz (left panel), full pressure (middle panel) and hydrostatic pressure (right panel) at the crash gridpoint. The black, red and blue curves represent the three lowest model levels km, km-1, km-2 respectively.

All the variables that are used to compute w are investigated. An unrealistic full pressure (>5000 hPa) is identified at the model lowest level at many acoustic steps (about 200 seconds) before the model crash, while the hydrostatic pressure and other variables remain to be normal (Fig. 1). The problem in the full pressure is further tracked back to the presence of an extreme small depth thickness at the lowest model layer where δz is very close to zero (Fig. 1). GFSv16 has 127 vertical layers with the lowest layer being about 20 m thick on average. It is unphysical for δz reaching to zero.

The forward-in-time advective processes are performed to generate the partially-updated geopotential height *z* before the non-hydrostatic adjustment in the FV3 dynamics. Note that the update of *z* through advection processes does not directly solve an equation for the volume of a grid cell, and it is forward-in-time as the sum of the advective height flux along the Lagrangian interfaces and the vertical distortion of the surfaces by the gradient of *z*. To solve *z* on the interfaces, the advecting winds are appropriately interpolated from layer means onto the layer interfaces by solving a tridiagonal system of equations based on the Parabolic Spline Method (PSM, Zerroukat et al. 2006) with high-order boundary conditions.

Figure 2 shows the time series of geopotential height at the break grid at the model lowest layers before and after the advection processes. The only evident change in terms of *z* with model integration is the increasing *z* at the model lowest level after advection, which is consistent with the decreasing of thickness depth seen in Figure 1.

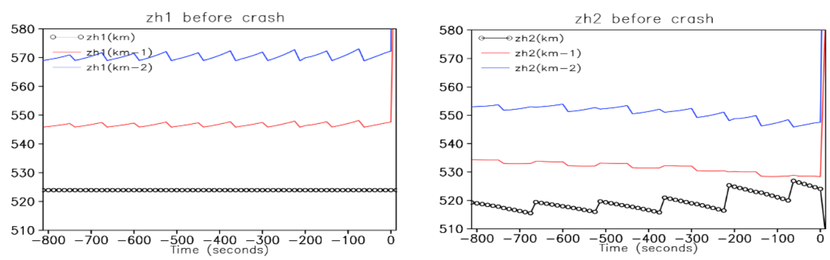

Figure 2. The time series of the geopotential height at the break grid at the model lowest three levels before (left panel) and after (right panel) the advection processes.

3. Potential solutions

An artificial limiter for the minimum thickness depth is defined in the FV3 dynamic code. This limiter is used with a value of 2 (meters) to enhance the monotonicity of height after the advection of *z*. We performed extensive sensitivity tests to stabilize the model with many other options and found that increasing the value of minimum thickness depth from 2 to 6 is the most effective and simple way to avoid model crashes. More importantly this fix has a very little impact on forecast skill. This temporary fix was implemented in GFSv16 to meet the model upgrade schedule.

Since the model instability issue likely originated from the advection of *z* at the model lowest level, we proposed to use zero-gradient boundary conditions (BCs), instead of high-order BCs, to reconstruct horizontal winds at the interfaces from layer means with PSM. The new BCs do not impact interior winds, except for smaller vertical gradients in the lowest model layers in the vertical. With the new BCs, all the originally failed cases were run successfully for 16 days in forecast length without applying the minimum thickness limiter.

The impact of this new method on model forecast was investigated in GFS.v16, the FV3-based limited area model and idealized mountain ridge experiments. Results show that this new method can effectively solve the model instability issues while incur little impact on forecast performance and the numerical solutions of idealized mountain waves.

References

Lin S.-J. and R. B. Rood, 1997: An explicit flux-form semi-Langrangian shallow-water model on the sphere, *Q. J. R. Meteorol. Soc*., 123， 2477-2498.

Putman, M. and S.-J. Lin, 2007: Finite-volume transport on various cubed-sphere grids. *J. Comp. Phys.*, 227, 55-78.

Zerroukat, M., Wood, N., and Staniforth, A. 2006: The Parabolic Spline Method (PSM) for conservative transport problems. *Inter. J. Num. Meth. in Flu.,* 51, 1297-1318.

Acknowledgement: We thank GFDL's support especially Lucas Harris, Xi Chen and Linjiong Zhou and EMC colleagues Fanglin Yang, Sajal Kar et al. for their insightful suggestions and discussions.